Plasma properties measurements of parallel-plane electrodes in argon by coupling OES and PLIF

Wang, Fangyi, Zhang, Shaohua, Yu, Xilong

Fangyi Wang, Shaohua Zhang, Xilong Yu, "Plasma properties measurements of parallel-plane electrodes in argon by coupling OES and PLIF," Proc. SPIE 11780, Global Intelligent Industry Conference 2020, 1178016 (18 March 2021); doi: 10.1117/12.2590211

SPIE.

Event: Global Intelligent Industry Conference 2020, 2020, Guangzhou, China

Plasma properties measurements of parallel-plane electrodes in Argon by coupling OES and PLIF

WANG Fangyi, ZHANG Shaohua, YU Xilong

（State Key Laboratory of High Temperature Gas Dynamics, Institute of Mechanics, Chinese Academy of Sciences, Beijing 100190, China
School of Engineering Science, University of Chinese Academy of Sciences, Beijing 100049, China）

ABSTRACT

Plasma properties are diagnosed in parallel-plane electrodes under 1-15 kPa within input power of 0-25 W by coupling Optical Emission Spectroscopy (OES) and Planar Laser-induced fluorescence (PLIF). Electron excitation temperature (T_e), electron density (N_e) are obtained based on the intensities and broadenings of atomic and ionic spectral lines of argon. The spatial resolution of T_e and N_e are measured by a high-precision setup based on fiber. At the gas pressure of 1 kPa, T_e reaches maximum of 8.745×10^3 K while the peak of N_e appears in 15 kPa, is 3.237×10^{16} cm^{-3}. Besides, spatial distribution of $1s_5$ metastable atoms (Ar^M) with transition scheme $4s(^2P^0_{3/2})_2$-$4p'(^2P^0_{1/2})_1$-$4s(^2P^0_{3/2})_1$ are revealed by PLIF, as a complementary of plasma properties. The number density of Ar^M also shows a larger number density in 15 kPa. Combined with OES, T_e, N_e and number of Ar^M are higher around the surface of anode within discharge area. The current experimental results are demonstration of optimal plasma state under different external parameters and validation of relevant discharge models.

Key words: Optical Emission Spectroscopy; Planar Laser-induced Fluorescence; Plasma properties; Metastable atoms

1. INTRODUCTION

Low-pressure discharge plasmas has a wide range of applications, such as surface modification, lighting applications, the fabrication of microelectronic devices and so on [1-5]. Recent years, non-equilibrium plasma, which produced by inert gas (argon, nitrogen, etc.), has applied to assisted combustion field. It has shown great potential of improving combustion performance and has become a topic of great interest [6-9]. However, the physical behavior of such discharges is characterized by a large variety of basic mechanisms and the complex interaction of the physical and chemical processes involved. Besides, plasma is composed of electron, ion, ground atom, metastable atom and other neutral particles. All of them greatly depends on gas pressure, discharge geometry, cathode material and other external

Global Intelligent Industry Conference 2020, edited by Liang Wang, Proc. of SPIE
Vol. 11780, 1178016 · © 2021 SPIE · CCC code: 0277-786X/21/$21
doi: 10.1117/12.2590211

parameters that can be complicated[10]. Therefore, it is necessary to measure plasma properties quantitatively in order to monitor the response of plasma under modifiable working conditions. These basic researches will promote the application of non-equilibrium plasma to more domains.

Considering the measurement accuracy, non-intrusive optical diagnosis are carried on in order to avoid the interference to electric field. As a frequently used technique among kinds of non-intrusive plasma diagnostic methods, Optical Emission Spectroscopy (OES) only based on moderate spectroscopic equipment, has a short response time and easy to implement. It has been proved to be a convenient way for determination of electron densities and temperature, which is essential for understanding discharge microscopic processes [11-13]. Besides, metastable species formation are vital to electron energy-loss mechanisms, which are measured by Planar Laser-induced Fluorescence (PLIF) [14-17]. The two-dimensional fluorescence signal is unaffected by the emission of excited atoms.

In order to seek controllable access to low-temperature plasma that meets demand, comprehensive information about the response of plasma to external conditions should be understand. Current work are aimed at discharge behaviors between parallel-plane electrodes based on plasma properties. By building a constant volume discharge device, this paper deals with the plasma properties between parallel-plane electrodes in argon under 1-15 kPa within input power of 0-25 W. Electron density (N_e), electron temperature (T_e) are obtained by OES and distribution of Ar^M in $1s_5$ level is measured by PLIF. Simultaneous measurement are achieved by accurate timing controlling between two diagnostics.

2. EXPERIMENTAL SETUP

In Fig.1, a discharge chamber of constant volume with optical windows on three sides were established and a precision pressure gauge were mounted on top. Argon gas flowed slowly from the incoming pipeline through the chamber to the vacuum pump in order to keep an invariable pressure. Discharge configuration was set as parallel plane made of copper due to its good conductivity. Distance between two same planes, which is 28 mm long and 2 mm thick, was fixed at 8 mm. An AC power (Coronalab CTP-2000K, Nanjing, CN) was applied as discharge power supply with a frequency maintained at 5 kHz. The waveform of voltage and current were recorded by probes (Rigol RP5600A 10:1 probe 600 MHz) to an oscilloscope (Rigol DS6064 Digital Oscilloscope 4 channel 600 MHz 5 GSa/s) as Fig.1(a) shown.

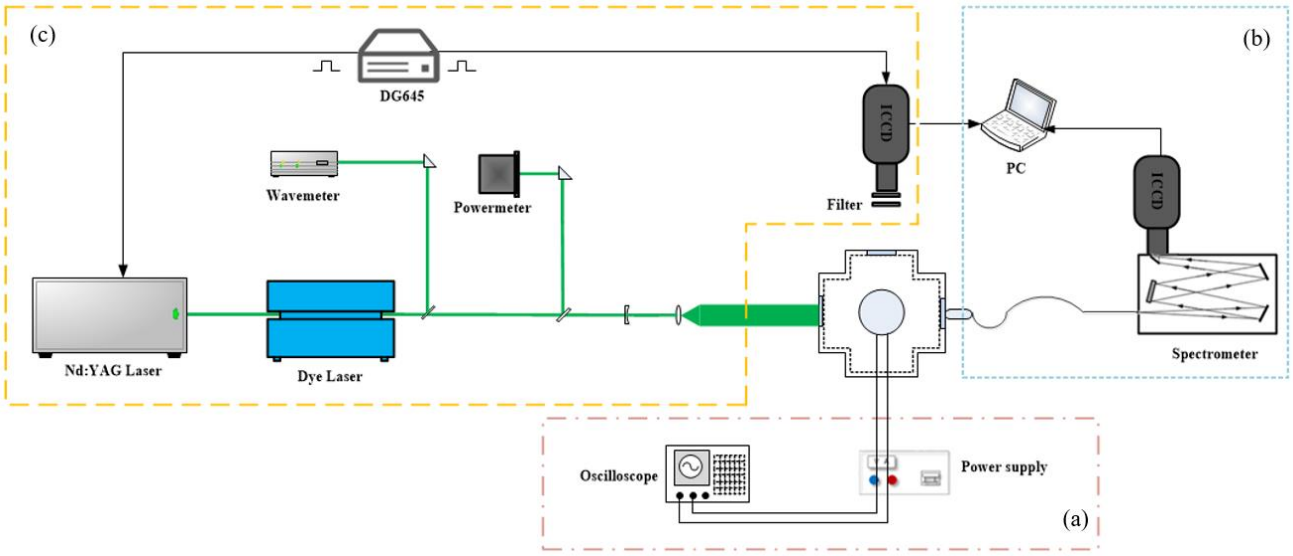

Fig.1. Experimental setup.

The OES system were calibrated in both wavelength and intensity before measuring. Besides, the instrumental broadening was also calibrated by IntelliCal apparatus (Princeton Instruments). Optical signal was collected through the fiber (TB-UV1000-TB-L2, Beijing Scitlion Technology CORP, LTD) into the 30-μm entrance slit of a 0.5-m spectrometer (Spectrapro HRS-500, Princeton Instruments) as Fig.1(b) shown. Noting that the fiber with spatial resolution has a single column of 4 fiber optic bundles, each 1 mm diameter. The emission signal was captured by an ICCD (PI-MAX 4, Princeton Instruments) with a gate width of 200 μs. The wavelength range and typical spectra lines from argon atoms and ions were displayed in Fig.2.

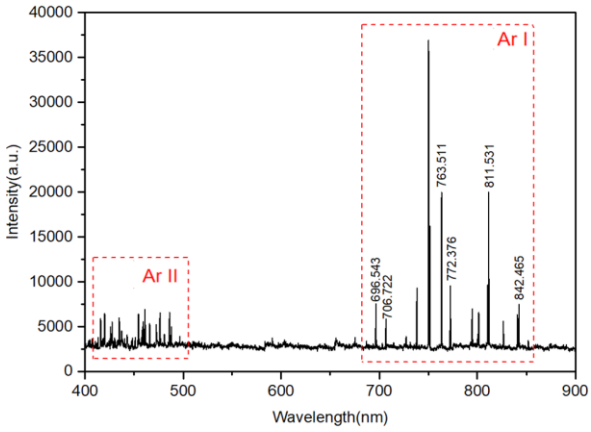

Fig.2. A typical spectra of Ar in glow discharge.

In PLIF experimental setup shown in Fig.1(c), transition scheme of $4s(^2P^0_{3/2})_2$-$4p'(^2P^0_{1/2})_1$-$4s(^2P^0_{3/2})_1$ was selected due to the metastable state $1s_5$ (In Paschen's notation) had the lowest excited-energy and a reported lifetime up to tens of seconds. Its number density could also approximate the neutral ground state with a higher signal-to-noise (SNR). Nd:YAG (Quanta-Ray Pro250, Spectra-Physics) laser was used to pump the dye laser (Precisionscan, Sirah). The tuning of the laser wavelength was achieved with the help of Pyridine 1 (dye) and frequency-doubling crystal. Right in front of electrode module, another ICCD was placed to detect the fluorescence signal through the optical window that has an effective measuring diameter of 30 mm. A narrow band filter (central wavelength of 730 nm with 10 nm half-band width) was installed in front of the camera lens.

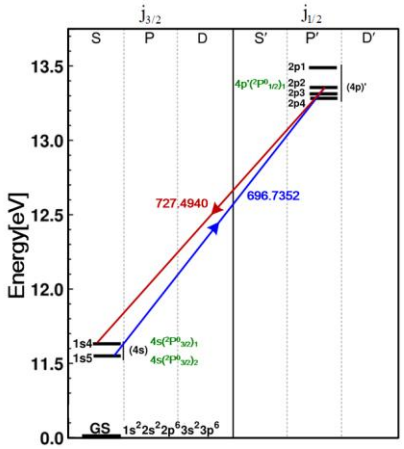

Fig. 3. Energy level diagram of Ar-I LIF schemes.

Before scanned in excitation wavelength with the $1s_5$ scheme to determine appropriate parameters, it was necessary to ensure the laser power in the linear excitation region since saturation would disable some experimental data. 70 mJ/pulse was still in the linear excitation region of laser energy versus LIF signal intensity as presented in Fig.4. 30 mJ/pulse was selected as the laser power for its good SNR and less statistical jitters.

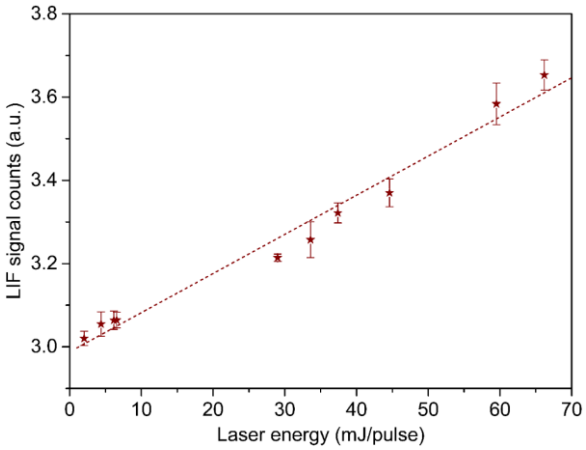

Fig. 4. LIF signal intensity as a function of laser energy.

The time synchronization sequence of OES and PLIF are achieved by with a digital delay generator (Stanford, DG645). Note that the selected working conditions in this experiment are listed in Table.1.

Table.1. Working condition in experiment.

Gas Pressure (kPa)	Input Power (W)					
1	1.0	2.3	4.5	8.1	12.6	17.4
2	1.4	4.4	7.4	10.3	13.4	17.8
5	2.1	5.8	8.7	12.1	17.3	23.1
10	2.5	6.0	9.1	12.7	16	20.5
15	2.3	5.1	8.2	10.8	13.6	18.4

3. RESULTS AND DISCUSSION

3.1 Electron temperature

Rates of reactions, which induced by electron collisions, were depend on the energies of the electrons that drive them directly. Electron temperature is thus motivated by the characterization of electron energy distribution function in order to predict the plasma behavior. Provided that the plasma in LTE, i.e. the populations of atoms, ions of Ar at the different energy levels follow a Boltzmann distribution. Relative evidence were presented in next section. T_e were determined by the following equation:

$$ln\left(\frac{I\lambda}{A_{ki}g_k}\right) = -\frac{E_k}{kT_e} + C$$

Where I is the relative intensity of spectral lines, λ is the wavelength, k is Boltzmann's constant. g_k and E_k are the statistical weight and the energy of the upper level respectively, A_{ki} is the Einstein transition probability.

In Fig.5, T_e drops with increasing input power as illustrated when gas pressure keeps constant. Amplitude of voltage decreases in proportion to the current under all conditions, which is called negative resistance characters. If the input power is disassembled to following parts: greater current density brings about the contraction of electrode sheath, which accelerates electron-quenching; charged particle owns higher velocity because voltage as well as the significance of edge effect grows. Reduction of voltage as input power rises contributes to the result of T_e presented in Fig.5. When input power keeps constant, large value of pressure leads to a more frequently collisions between electrons and neutral particles. Reduced free path has played a more dominated role as the pressure rises. Therefore, the maximum of electron temperature appears at 1 kPa is 8.745×10^3 K.

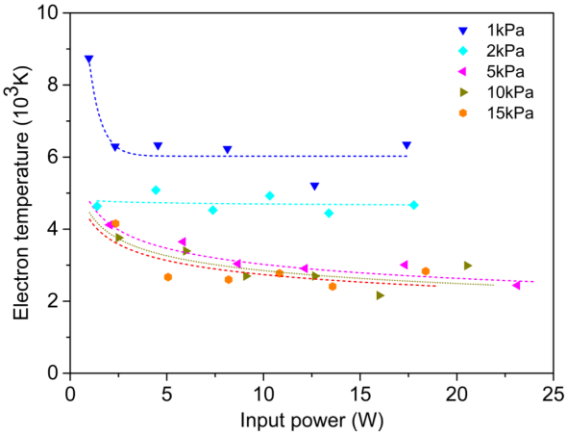

Fig. 5. Electron temperature as a function of gas pressure and input power.

3.2 Electron density

It is generally known that the density and energy distribution of electrons are important in controlling sensitivity in optical emission and mass spectrometric applications of glow discharges. Plasma-broadened and shifted spectral line profiles have been used for a number of years as a basis of electron number density diagnostic. The spectral lines emitted from plasma are subject to various broadening mechanisms. Among them, natural and resonance broadening are generally negligible in plasma with high electron density. The full width at half maximum (FWHM) follow Voigt profile, which is a convolution of Gaussian and Lorentzian profiles. After deduct the instrumental broadening from FWHM, Doppler and instrumental broadening follow Gaussian profile, Van der Waals and Stark broadening follow Lorentzian profiles. Lorentzian profile can be obtained by applying deconvolution to FWHM, thus the stark broadening will be solved after subtract the Van der Waals broadening. Spectral line in 696.5432 nm of Ar I is chosen to diagnose the electron density because it is a strong and comparatively, well isolated spectrum line of the neutral argon. It takes the form:

$$\Delta\lambda_{stark} = 2\times[1+1.75\times10^{-4}N_e^{1/4}\alpha\times(1-0.068N_e^{1/6}T_e^{-1/2})]\times10^{-16}\omega N_e$$

Where α is the static ion-broadening parameter, ω is electron impact half-width [18]. So far, we are able to use the criterion: $N_e \geq 1.4\times10^{14} T_e^{1/2} (\Delta E)^3$ from MCWHIRTER's work [19] to check the assumption state of LTE.

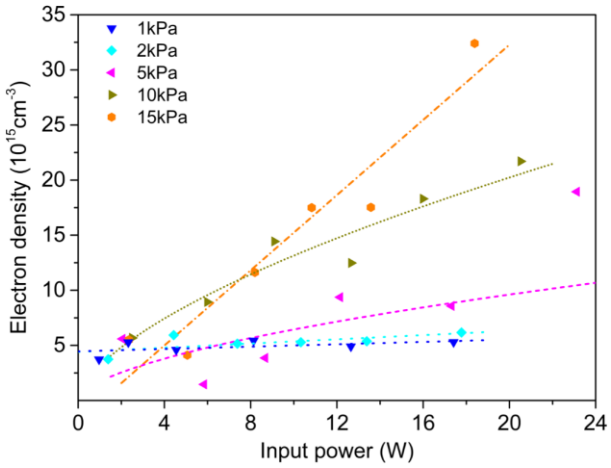

Fig. 6. Electron density as a function of gas pressure and input power.

In Fig.6, N_e have shown a reverse trend to T_e (Fig.5) under same external parameters. The maximum of electron density appears at 15 kPa is 3.237×10^{16} cm^{-3}. Electron cooling effect, which means most kinetic energy of electrons have transferred to other electrons and converted to internal energy of neutral particles, are accompanied by reduced T_e and incremental N_e.

3.3 Distribution of Ar^M

The information obtained by PLIF is able to support the OES data, for example some features of excitation processes of 2p atoms can be traced to the behavior of spectral lines. Consequently, LIF of Ar^M (the excited population of Ar atoms) in the plasma region is performed as a complement of flow distribution.

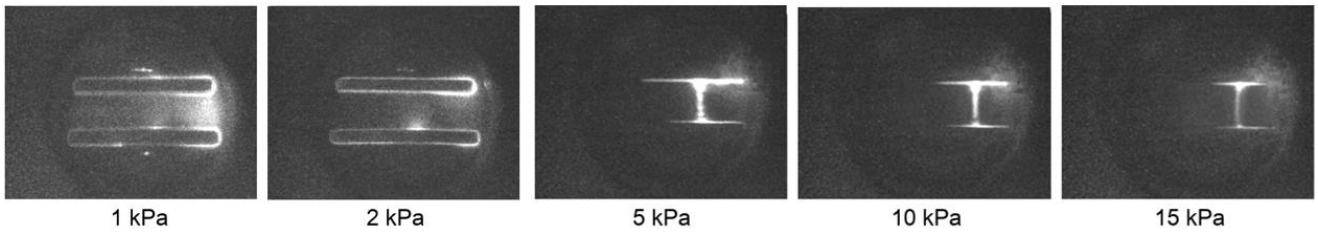

FIG. 7. Spatial distributions of Ar metastable under different gas pressures.

An illustrative set of photographs for the spatial distributions of $1s_5$ metastable density at various gas pressures are shown in Fig.7. When the gas pressure adjust to 1 kPa, electrodes spots are formed as Fig.7 shown. Besides, the head of electron avalanche and arc constriction are distinguished clearly in 5 kPa based on streamer theory.

The fluorescence figures have displayed that most of $1s_5$ metastable atoms during discharge in view of the overall situation. In general, excited atom population distribution is affected by N_e and T_e, mainly. However, when T_e less than

1.5eV in this work, its effect on the distribution is very small compared with N_e, whose range of variation is several orders of magnitude greater. Increasing pressure leads to a consequent decrease in direct ionization contribution with respect to the step ionization, just as other previous work [20] demonstrated through reaction rates of dominant kinetic processes. Therefore, the number density of Ar^M changes along with electron density, which are proved exactly by the comparison between OES and PLIF.

4. CONCLUSIONS

In this work, both Optical Emission Spectroscopy (OES) and Planar Laser-induced Fluorescence (PLIF) techniques are applied for simultaneous determination of plasma properties in parallel-plane copper electrodes within an argon discharge. Under the experimental conditions of input power range from 0-25 W, gas pressure 1-15 kPa, electron temperature and electron density were obtained simultaneously by OES, provided a reliable result for simulation model. When gas pressure rises, electron temperature goes down gradually while electron density shows an opposite way, taking it by and large. Moreover, the two-dimensional distribution of Ar^M have been studied using PLIF imaging spectroscopy.

Mutual corroboration between OES and PLIF reveals the reliability of our conclusion, which have confirmed quantitative plasma properties can be obtained effectively through this experimental setup. Experimental results here displayed can also be references in developing reliable models and precise simulations of discharge with quantitative physical parameters. Fundamental data from this work are prepared for on-line measurements, which is a necessary stage for controlling plasma state with and predicting the optimal external conditions.

ACKNOWLEDGEMENTS

This work was performed with support from the National Science Foundation of China (Grant no.11672359, no.11872368, no.11927803).

REFERENCES

[1] Escoffier C. l., Maguire P., McAdams E., et al., "Surface Modification of Silver Thin Films Using Low Power Chlorine Plasmas," ELECTROCHEMICAL AND SOLID STATE LETTERS abbreviation. 4, H31-H33 (2001).

[2] Popelka A., Bhadra J., Abdulkareem A., et al., "Fabrication of flexible electrically conductive polymer-based micropatterns using plasma discharge," Sensors and Actuators A: Physical abbreviation. 301, 111727 (2020).

[3] Chu P. K., Chen J. Y., Wang L. P., et al., "Plasma-surface modification of biomaterials," Materials Science and Engineering: R: Reports abbreviation. 36, 143-206 (2002).

[4] Foest R., Kindel E., Ohl A., et al., "Non-thermal atmospheric pressure discharges for surface modification," Plasma Phys Contr F abbreviation. 47, B525-B536 (2005).

[5] Adamovich I., Baalrud S. D., Bogaerts A., et al., "The 2017 Plasma Roadmap: Low temperature plasma science and technology," Journal of Physics D: Applied Physics abbreviation. 50, 323001 (2017).

[6] Yang S., Nagaraja S., Sun W., et al., "Multiscale modeling and general theory of non-equilibrium plasma-assisted ignition and combustion," J Phys D Appl Phys abbreviation. 50, (2017).

[7] Sun J., Chen Q., Guo Y., et al., "Quantitative behavior of vibrational excitation in AC plasma assisted dry reforming

of methane," Journal of Energy Chemistry abbreviation. 46, 133-143 (2020).
[8] Starikovskiy A., "Physics and chemistry of plasma-assisted combustion," Philosophical Transactions of the Royal Society a-Mathematical Physical and Engineering Sciences abbreviation. 373, (2015).
[9] Liu X., He L., Chen Y., et al., "EMISSION CHARACTERISTICS OF AVIATION KEROSENE COMBUSTION IN AERO-ENGINE ANNULAR COMBUSTOR WITH LOW TEMPERATURE PLASMA ASSISTANCE," Thermal Science abbreviation. 23, 647-660 (2019).
[10] Eliseev S. I., Kudryavtsev A. A., Liu H., et al., "Transition from glow microdischarge to arc discharge with thermionic cathode in argon at atmospheric pressure," IEEE Transactions on Plasma Science abbreviation. 44, 2536-2544 (2016).
[11] Mochalov L., Dorosz D., Kochanowicz M., et al., "Optical emission spectroscopy of lead sulfide films plasma deposition," Spectrochimica Acta Part a-Molecular and Biomolecular Spectroscopy abbreviation. 241, (2020).
[12] Kobayashi T., Yoshinuma M., Ida K., "Two-dimensional beam emission spectroscopy for hydrogen isotope negative neutral beam in Large Helical Device," Plasma Phys Contr F abbreviation. 62, (2020).
[13] Arora P., Cho J., Cervantes R., et al., "Glow discharge-optical emission spectroscopy for in situ analysis of surfaces in plasmas," Journal of Vacuum Science & Technology A abbreviation. 38, (2020).
[14] Gao J., Zhu J., Ehn A., et al., "In-Situ Non-intrusive Diagnostics of Toluene Removal by a Gliding Arc Discharge Using Planar Laser-Induced Fluorescence," Plasma Chem Plasma P abbreviation. 37, 433-450 (2017).
[15] Schmidt J. B., Jiang N., Ganguly B. N., "Nitric oxide PLIF measurement in a point-to-plane pulsed discharge in vitiated air of a propane/air flame," Plasma Sources Sci T abbreviation. 23, (2014).
[16] Vorac J., Synek P., Dvorak P., et al., "Time- and space-resolved LIF measurement of the concentration of OH radicals generated by surface barrier discharge emerging from liquid water," Plasma Sources Sci T abbreviation. 28, (2019).
[17] Wang H., Liu J., Wang Z., et al. Investigation of Vacuum Arc Extinction Process by Planar Laser-Induced Fluorescence. In: [Proceedings of the 2018 28th International Symposium on Discharges and Electrical Insulation in Vacuum], pp. 313-315 (2018).
[18] Griem H. R., [Plasma spectroscopy]. (1961).
[19] Huddlestone R. H., Leonard S. L., "Plasma diagnostic techniques," Plasma Diagnostic Techniques abbreviation., (1965).
[20] Zhu X. M., Pu Y. K., Balcon N., et al., "Measurement of the electron density in atmospheric-pressure low-temperature argon discharges by line-ratio method of optical emission spectroscopy," J. Phys. D-Appl. Phys. abbreviation. 42, 5 (2009).